Expression of genes related to apoptosis, cell cycle and signaling pathways are independent of *TP53* status in urinary bladder cancer cells

Glenda N. da Silva · Adriane F. Evangelista · Danielle A. Magalhães ·
Cláudia Macedo · Michelle C. Búfalo · Elza T. Sakamoto-Hojo ·
Geraldo A.S. Passos · Daisy M. F. Salvadori

Abstract Urinary bladder cancer is the fourth most common malignancy in the Western world. Transitional cell carcinoma (TCC) is the most common subtype, accounting for about 90% of all bladder cancers. The *TP53* gene plays an essential role in the regulation of the cell cycle and apoptosis and therefore contributes to cellular transformation and malignancy; however, little is known about the differential gene expression patterns in human tumors that present with the wild-type or mutated *TP53* gene. Therefore, because gene profiling can provide new insights into the molecular biology of bladder cancer, the present study aimed to compare the molecular profiles of bladder cancer cell lines with different *TP53* alleles, including the wild type (RT4) and two mutants (5637, with mutations in codons 280 and 72; and T24, a *TP53* allele encoding an in-frame deletion of tyrosine 126). Unsupervised hierarchical clustering and gene networks were constructed based on data generated by cDNA microarrays using mRNA from the three cell lines. Differentially expressed genes related to the cell cycle, cell division, cell death, and cell proliferation were observed in the three cell lines. However, the cDNA microarray data did not cluster cell lines based on their *TP53* allele. The gene profiles of the RT4 cells were more similar to those of T24 than to those of the 5637 cells. While the deregulation of both the cell cycle and the apoptotic pathways was particularly related to TCC, these alterations were not associated with the *TP53* status.

Authors contributions "All authors reviewed the manuscript. GNS was responsible for the study design and interpretation of the data; performed most of the experiments and wrote the manuscript. AFE was responsible for constructing the gene networks. DAM and CM conducted the cDNA microarray experiments. MCB conducted the real-time qPCR experiments. GASP and ETSH contributed to the interpretation of data and provided critical readings of the manuscript. DMFS contributed to the study design and interpretation of the data, as well as provided a critical reading of the manuscript."

G. N. da Silva (✉) · D. M. F. Salvadori
Faculdade de Medicina de Botucatu, Botucatu Medical School,
UNESP—São Paulo State University, Botucatu, SP 18618-000,
Brazil
e-mail: nicioli@fmb.unesp.br

A. F. Evangelista · D. A. Magalhães · C. Macedo ·
E. T. Sakamoto-Hojo · G. A.S.Passos
USP—University of São Paulo, Faculty of Medicine, Ribeirão
Preto, SP, Brazil

M. C. Búfalo
UNESP—São Paulo State University, Biosciences Institute,
Botucatu, SP, Brazil

E. T. Sakamoto-Hojo
USP—University of São Paulo Department of Biology
(FFCLRP), Ribeirão Preto, SP, Brazil

G. A.S.Passos
USP—University of São Paulo Faculty of Dentistry, Ribeirão
Preto, SP, Brazil

Background

Urothelial carcinoma is a significant health problem and is the fourth most common malignancy in the Western world [1]. The majority of patients present superficial disease (i.e., tumors that do not invade the muscularis mucosa), and approximately 70% of patients develop disease recurrence with 10–40% of cases ultimately progressing to muscle-invasive disease [2, 3]. Histologically, transitional cell

carcinoma (TCC) is the most common subtype and represents nearly 90% of all bladder cancers[4].

Urothelial cancer has been described as a tumor type in which the *TP53* gene is frequently mutated [5]. The *TP53* gene plays an essential role in regulating the cell cycle and apoptosis and therefore contributes to both cellular transformation and malignancy [6]. Moreover, p53 is a DNA-binding protein that contains transcription, DNA-binding, and oligomerization activation domains; furthermore, p53 functions as a tumor suppressor [7]. However, little is known concerning the differential gene expression patterns of human tumors presenting either wild-type or mutated *TP53*. Sanchez-Carbayo et al. [8] have observed that bladder tumor cells assemble based on their molecular alterations in relation to the *TP5*3 and *RB* signaling pathways. Moreover, they observed that cells that harbor *TP53* mutations in exons 4 and 5, detectable pRB, and INK4A mutations cluster together and were distinguishable from those with *TP53* mutations affecting exons 7, 10, and 11, undetectable levels of pRB, and a wild-type INK4A locus. Similarly, another study demonstrated that *TP53* mutations frequently occur in the progression of bladder cancer; moreover, they identified a relationship between gelsolin and *TP53* status, tumor staging, and clinical outcome [9].

In the post-genome era, high-throughput methods have enabled investigators to perform comprehensive analyses of molecular activities in different cell types, which may lead to greater understanding of carcinogenesis and tumor development. In this context, the DNA microarray has become the preferred method for the large-scale analysis of gene expression [10]. The DNA microarray is a molecular technology that enables identification of gene interactions from experimental data through computational analysis [11]. The elucidation of the molecular events involved in tumorigenesis has led directly to the discovery and application of novel biological markers, including some predictive biomarkers for bladder tumors [8, 9]. Some investigators have shown, for instance, that repression of the hTERT (human telomerase reverse transcriptase) transcript decreases the expression of the *EGFR* gene at the mRNA and protein levels, supporting the hypothesis that hTERT promotes the growth of tumor cells by mechanisms independent of telomere lengthening [12]. On the other hand, Kikuchi et al. [13] have also shown that expression data can easily distinguish two major histological types of non-small cell lung cancer, adenocarcinoma and squamous cell carcinoma. Subsequent analysis of the adenocarcinomas identified genes whose expression levels could separate cases with lymph-node metastasis from those without metastasis. Additionally, Staege et al. [14] have detected differences between the gene-expression profiles of chemotherapy-resistant and -sensitive Hodgkin's lymphoma cells.

At present, *TP53* sequences and gene expression profiles associated with *TP53* status can be characterized in a high-throughput manner. Therefore, in the present study, we aimed to better characterize bladder cancer cell lines by gene profiling and gene networks to validate new targets involved in tumor progression using cDNA microarray and quantitative real-time PCR (qRT-PCR) technologies.

Materials and methods

Cell lines

The established cell lines RT4, 5637, and T24 from human bladder TCCs were obtained from the Cell Bank of the Federal University of Rio de Janeiro, Brazil. The 5637 cells, obtained from a moderately differentiated tumor, contain two mutations in the *TP53* gene, one at codon 280 (Arg > Thr) and the other at codon 72 (Arg > Pro) [9, 15, 16]. The T24 cells, obtained from a high-grade tumor, display a *TP53* allele encoding an in-frame deletion of tyrosine 126 [9, 15]. No specific mutations are found in the RT4 cells, which is a cell line established from a low-grade papillary bladder tumor [15]. The cells were cultured following standard procedures [17].

RNA extraction

All cells were grown and harvested at 80–90% confluence, after no more than six passages in culture, for the extraction of total RNA using the mirVana kit (Ambion, Applied Biosystems) according to the manufacturer's instructions. The extracted RNA was stored at –80°C. The integrity of the samples was evaluated by denaturing agarose gel electrophoresis under standard conditions.

cDNA microarray and gene expression analysis

Analyses of the gene expression profiles were performed using glass slide microarrays containing 4,500 sequences (spotted in duplicate) from the human IMAGE cDNA library Consortium (http://image.llnl.gov/image/), which were kindly provided by Dr. Catherine Nguyen (INSERM-CNRS, Marseille, France) and prepared according to the protocol described by Hegde et al. [18]. The microarrays were prepared using type 7 silanized glass slides (Amersham Biosciences, England) and a Generation III Array Spotter (Amersham-Molecular Dynamics) according to the manufacturer's instructions. The cDNA complex probes were prepared from samples of the cell lines, and reverse transcription was carried out with 10 μg of total RNA/

sample in the presence the Cy3 or Cy5 fluorochromes (CyScribe Post Labeling Kit, Amersham Biosciences) and oligo dT12–18 primers. A pooled reference design was chosen. More specifically, each array was hybridized with the same reference sample (prepared from three different cell lines: U343 MG-a glioma, HeLa, and Jurkat cells) labeled with Cy5, while the experimental samples (control or treated) were labeled with Cy3. The reference sample was used in the normalization procedure. Hybridizations were performed for 15 h using an automated system (Automatic Slide Processor, Amersham Biosciences). The hybridization signals were captured using a Generation III laser scanner (Amersham Biosciences).

Image quantification was performed using the Spot software (http://www.tm4.org/spotfinder.html) [19]. Filtering, normalization, and data analysis were performed using the R Statistical Environment [20] according to the instructions and with the KTH package (http://www.bio tech.kth.se/molbio/microarray/) [21]. The background for each feature was subtracted from the foreground value. Furthermore, each spot was evaluated on the basis of its circularity and the deviation between its median and the mean. Spots with irregular circularity or large differences between the mean and their median values were considered unreliable. Subsequently, the print-tip Lowess normalization method was applied, and the M values were rescaled by the MAD (median absolute deviation) value [22]. The normalized data were exported to the MEV format and analyzed using the MEV software (http://www.tm4.org/mev.html) [23], which was used to perform statistical analyses and hierarchical clustering. For the clustering procedures, normalized genes were median-centered. The information regarding gene locations and biological functions was obtained from S.O.U.R.C.E. (http://smd-www.stanford.edu/cgi-bin/source/sourceSearch) [24], NCBI (http://www.ncbi.nlm.nih.gov/) [25] and FATIGO (http://babelomics.bioinfo.cipf.es/) [26].

For data analysis, ANOVA (uncorrected $P < 0.10$) was used. The significance analysis of microarrays method (SAM) (FDR < 0.05) was applied for those genes identified by ANOVA, and multiclass comparisons were performed. The SAM method, which assigns a score to each gene on the basis of change in gene expression relative to the standard deviation of repeated measurements, was used for each independent experiment. The SAM method uses permutations of the repeated measurements to estimate the percentage of genes identified by chance, which is the false discovery rate (FDR), and constructs a scatter plot displaying the induced and repressed genes [27]. A complete file providing all of the genes and ESTs present in the microarrays used in this study, as well as the experimental conditions, are available at MIAME public database: Array Express accession E-MEXP-2859.

Gene network analysis

The GeneNetwork v1.2 algorithm was used to compare the median values for the different gene expressions in cases where the standard deviations did not overlap. The software implementing this algorithm can be obtained from http://idv.sinica.edu.tw/hchuang/GeneNetwork1.2Setup.exe [28]. The objective was to compute a network that established relationships between genes. Bayesian interpolation was used for the network organization. The parameters utilized were based on the probabilities for a hypothetical population of 200 individuals and a mutation rate of 0.02. All utilized networks were stabilized. To organize networks with only the genes whose expression values were significant, normalized values for the induced and repressed genes obtained from the SAM statistical analysis were used. Genes found in both tumor grades establishing interactions with *TP53* and other sequences were considered.

Validation of gene expression data by quantitative real-time pcr

cDNA synthesis

The differential expression of two genes randomly selected from the microarray analysis (*ANLN* and *S100P*) was validated by real-time PCR using the TaqMan system (Applied Biosystems, USA). *ANLN* and *S100P* were selected because of their participation in cancer progression. The *TP53* gene expression was also studied. Total RNA (1 μg) from the cell lines was reverse transcribed using 6 μl of random hexamer primer (10X), 6 μl of reaction buffer (10X), 2.5 μl of dNTPs (25X), and 3 μl of MultiScribe enzyme (50U/μl) (High Capacity, Applied Biosystems, USA). This mixture was incubated at 25°C for 10 min and then at 37°C for 2 h, and it was then kept at 4°C. Subsequently, each cDNA was stored at –20°C.

Quantitative real-time PCR

Each reaction tube contained 2 μl of cDNA template, 5 μl of Master Mix TaqMan 2X (Applied Biosystems), and 0.5 μl of 20× primers/probe (Assays-on-Demand Gene expression products, Applied Biosystems). *GAPDH* was used as the housekeeping gene. The PCR program consisted of the following steps: 2 min at 50°C, 10 min at 95°C, and 40 cycles of 15 s at 95°C, followed by 1 min at 60°C. Fluorescence data were collected during each annealing/extension step. The reactions were performed in an Applied Biosystems 7500 FAST Real-Time PCR System and were analyzed with SDS version 1.2.3 (Sequence Detection Systems 1.2.3, 7500 Real-Time PCR Systems, Applied Biosystems) software. For each PCR assay, a

negative (no template) control was processed for routine quality control. Assays were replicated in four independent experiments.

Standard curve and data analysis

To generate standard curves, four serial dilutions of the mRNA derived from the RT4 cell line were used. The first dilution (i.e., highest concentration) of the RNA standard was given the relative value 100, and the three other dilutions were given the relative values of 20, 4, and 0.8. The mRNA quantity in the samples was expressed relative to the standard curve. The results were analyzed by ANOVA and the Bonferroni multiple comparison test.

Results

Gene expression analysis by cDNA microarrays

ANOVA/SAM analyses with a false discovery rate of less than 0.05 revealed 756 differentially expressed genes among the three cell lines. Unsupervised hierarchical clustering of four cDNA microarray experiments showed that the gene profiling of the RT4 cells was more similar to that of T24 than to that of the 5637 cells (Fig. 1a). Using the FATIGO software, it was determined that these genes were mainly related to level 3 biological processes, including cell communication, cell death, cell cycle, cellular component organization, cell division, cell adhesion, and cell proliferation (Fig. 1b). From these 756 differentially expressed genes, seven important clusters of genes implicated in tumor recurrence, progression, and malignancy were selected for discussion (Table 1).

TP53 gene networks

For the *TP53* network analysis, 195 genes from the seven clusters were selected. Bayesian interpolation analyses of RT4 × 5637 (Fig. 2) and RT4 × T24 (Fig. 3) were performed to understand the mechanisms involved in carcinogenesis in the two mutated cell lines. The RT4 × 5637 network showed 183 differently expressed genes. Of these genes, 105 most likely modulate *TP53*, and 77 are likely modulated by the *TP53* gene. About one-third (66/183) of the genes are characteristic of and appear only in the RT4 × 5637 network, including *CDC40*, *OAS2*, *ATP1B3*, *PSMA1*, *MAP4K2*, and *TBXAS1*. The second network from the RT4 × T24 analysis showed 163 genes interacting with *TP53*, of which 61 most likely modulate *TP53* and 102 genes that are likely modulated by *TP53*. About one-fifth (33/162) of the genes are characteristic of the RT4 × T24 network, including *ITGA5*, *PDIA3*, and *GPR34*. Moreover,

the gene network analyses showed that *TP53* modulated *SP100* in the RT4 × T24 network and was modulated by *SP100* in the RT4 × 5637 analysis. Differential interactions were also found between *TP53* and *ANLN* in the two gene networks. However, the interaction between *ANLN* and *TP53* was likely indirect (i.e., through other genes) (data not shown).

S100P, ANLN, and TP53 gene expression

To validate the data obtained from the cDNA microarrays, two differentially expressed genes, *S100P* and *ANLN,* were tested by real-time qPCR. Additionally, the *TP53* expression was confirmed. The PCR efficiency of all genes was better than 83%.

The results showed an up-regulation of the *S100P* gene in RT4 when compared to the 5637 and T24 cell lines. The relative expression of the *S100P* gene in RT4, 5637, and T24 was 1, 0.06925, and 0.00172, respectively. The expression of the *ANLN* gene was down-regulated in RT4 and T24 compared to 5637, with relative expression levels of 1, 50.3575, and 3.71 in RT4, 5637, and T24, respectively. These data were similar to those obtained with the cDNA microarrays. The expression of *TP53* was significantly lower in T24 and RT4 than in the 5637 cells. The relative expression levels of *TP53* were 1, 28.985, and 0.4815 in RT4, 5637, and T24 cells, respectively (Fig. 4).

Discussion

Bladder cancer consists of a heterogeneous group of tumors that follow different pathways of development and progression. Further elucidation of the course of tumor progression and classification into distinct groups will likely have a significant effect on the management of this disease [29]. As a result, we aimed to characterize the gene expression profiles of three bladder cancer cell lines from different tumor grades and containing different *TP53* alleles using cDNA microarrays technique validated by real-time qPCR.

Unsupervised analysis showed no influence of *TP53* gene status on the hierarchical clustering for the three cell lines. From this analysis, RT4, a cell line derived from a superficial tumor with wild-type *TP53,* had a similar gene expression profile to that of T24, a cell line derived from an invasive tumor with mutated *TP53*; on the other hand, the 5637 cells, which were also derived from an invasive tumor moderately differentiated tumor and contain mutated *TP53*, had different gene expression profiles.

Several authors have shown that most of the mutations observed in human tumors abrogate or attenuate the binding of p53 to its consensus DNA sequence and,

Fig. 1 Gene expression profiling from transitional carcinoma cell lines (RT4, 5637, and T24) and the associated biological processes (level 3). **a** Heat map and seven selected clusters of unsupervised hierarchical clustering analysis from four replicates: the *red spots* indicate up-regulation, *green spots* indicate down-regulation, *black spots* indicate an absence of modulation, and *gray spots* indicate the absence of values; **b** Venn diagram mainly showing genes related to biological processes that are differentially expressed among the three cell lines. (Color figure online)
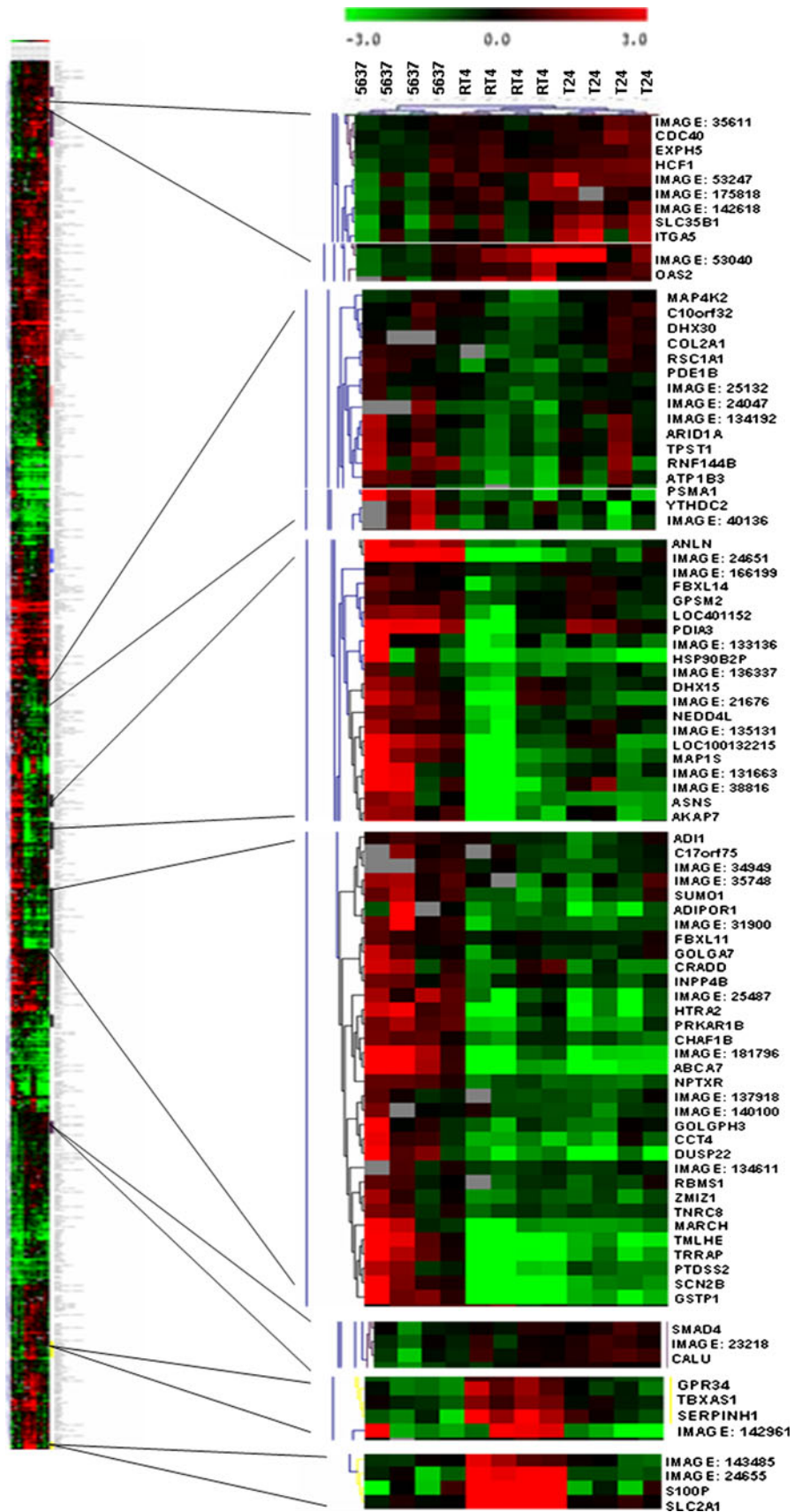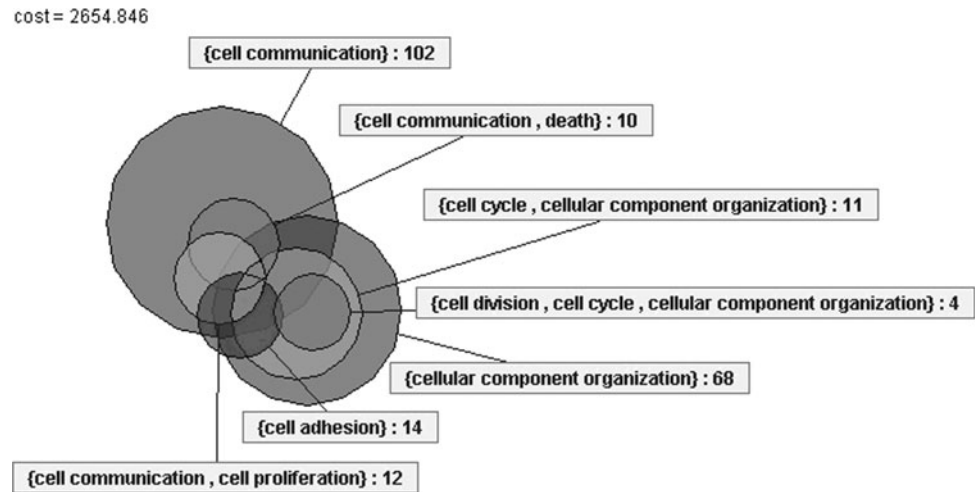
Fig. 1 continued

cost = 2654.846

{cell communication} : 102

{cell communication , death} : 10

{cell cycle , cellular component organization} : 11

{cell division , cell cycle , cellular component organization} : 4

{cellular component organization} : 68

{cell adhesion} : 14

{cell communication , cell proliferation} : 12

consequently, avoid the transcriptional activation of the p53 target genes. These mutations can result in partial or complete loss of the p53 [30] function. Several mutations were shown to confer new functions for mutant p53 that are independent of wild-type p53 [31]. These observations have several implications, including a possible heterogeneous clinical phenotype depending on whether p53 itself is mutated and on the site of the mutations or whether the p53 function is modified indirectly [32]. Moreover, some authors have suggested different responses to chemotherapy based on *TP53* status. As2O3, an ancient anticancer drug, suppresses the growth of the wild-type p53U87MG human glioma cells by regulating expression of genes involved in cell cycle arrest, stress and toxicity. On the other hand, this drug acts on mutant p53T98G cells by regulating genes related to Bcl-2, tumor necrotic factor receptor and ligand families [33].

Using bootstrapping methods, Sanchez-Carbayo et al. [8] have grouped bladder cancer cell lines based on their p53/pRB/INK4A pathways status. However, these authors have also observed that cells known to harbor mutations in exon 8 in the core domain (for instance, the 5637 cell line) were not included in the cluster described by the bootstrap technique. Thus, they have suggested that although the p53/pRB/INK4A pathways are important in the development and progression of bladder cancer, further investigations are necessary to identify other involved networks. On the other hand, when analyzing genome-wide expression profiles across different in vitro studies, it is difficult to find common signatures associated with the *TP53* mutations, which is likely due to variations in the type of mutant analyzed, the cellular system, and other technical variables [31]. In our study, the gene networks determined by Bayesian interpolation showed interactions among *TP53* and several other genes, suggesting that other pathways might be associated with the malignant phenotype. These

interactions were different in the two gene networks, but *TP53* was not a regulatory gene node in either network. For instance, in the 5637 gene network, the *S100P* gene was shown to likely stimulate *TP53*, while in the T24 gene network, the *S100P* gene seemed to be stimulated by the *TP53* gene.

When the results from the microarrays were classified according to gene functions, 406 of the 756 genes were those with no functional annotation. Of the remaining 350 genes, many were mainly involved in cellular communication, cell cycle, cell division, cell death, cellular component organization, cell adhesion, and cell proliferation, among other functions. These functions are essential for normal cellular processes, and when these pathways are altered, they can be implicated in the development and progression of bladder cancer.

Our results showed decreased expression of genes related to apoptosis in the RT4 and T24 cell lines compared to the 5637 cell line. The down-regulation of the *CRADD* and *HTRA2* genes indicates that apoptosis regulated by the activation of caspases could be compromised in these cells. The *HTRA2* gene acts as an inhibitor of IAP (inhibitor of apoptosis protein) [34], and CRADD promotes the interaction between the adaptor molecules and the prodomain of the initiator caspase 8 [35]. Additionally, differences in several signaling pathways, such as AMP kinase, JAK/ STAT3, and MAP kinase (p38 MAPK, ERK, JNK), were observed among the three cell lines. We detected downregulation of the *adipoR1* (involved in the AMP kinase pathway), *ABCA7* (involved in the ERK phosphorylation pathway), *DUSP22* (involved in the ERK and MAPK pathways), and *AKAP7* (involved in the second messengermediated signaling events) genes in the RT4 and T24 cells. Alterations in these pathways could trigger specific signals that might lead to uncontrolled cell growth, enhanced angiogenesis, inhibition of apoptosis, and genetic

Table 1 Differentially expressed genes among the RT4, 5637 and T24 cell lines selected from seven principal clusters and their related biological processes (level 3)

Name	Symbol	Clone ID	Expected Score (dExp)	Observed Score (d)	q-value (%)	Biological Process (GO[a])
Cell division cycle 40 homolog (S. cerevisiae)	CDC40	142587	0.7896793	1.1437857	0.0684965	Cell division
Integrin, alpha 5 (fibronectin receptor, alpha polypeptide)	ITGA5	135671	0.76935995	1.0256178	0.2516111	Cell adhesion, cellular component organization, cell communication
2'-5'-oligoadenylate synthetase 2, 69/71 kDa	OAS2	136508	0.37138805	1.2229251	0.0543942	Immune response
Mitogen-activated protein kinase kinase kinase 2	MAP4K2	37234	0.64513326	0.8204759	0.2516111	Cellular component organization, cell communication
ATPase, Na +/K + transporting, beta 3 polypeptide	ATP1B3	139611	0.141371	1.3908751	0.0197797	Establishment of localization
Thyroid hormone receptor-associated protein 3	THRAP3	133717	0.5918666	1.2702429	0.0440334	Cellular component organization, cell communication
Proteasome (prosome, macropain) subunit, alpha type, 1	PSMA1	134544	0.8704484	1.5289555	0.0143364	Catabolic process
Anillin, actin-binding protein	ANLN	28051	0.56963587	3.3534079	0.0	Cell division, cell cycle, cellular component organization
Protein disulfide isomerase family A, member 3	PDIA3	135083	0.45238787	2.0045464	0.0	Cellular component organization, cell communication, cell death
Neural precursor cell expressed, developmentally down-regulated 4-like	NEDD4L	24477	0.6218752	1.6108752	0.0	Cellular component organization
Microtubule-associated protein 1S	MAP1S	21951	0.52497995	2.0875363	0.0	Cellular component organization, cell death
Asparagine synthetase	ASNS	27208	0.3395816	1.503613	0.0135985	Nitrogen compound metabolic process
A kinase (PRKA) anchor protein 7	AKAP7	21643	0.32486033	1.7948898	0.0	Cell communication
Acireductone dioxygenase 1	ADI1	134466	0.12499792	0.95020324	0.2516111	Nitrogen compound metabolic process
SMT3 suppressor of mif two 3 homolog 1 (S. cerevisiae)	SUMO1	49768	0.70252854	1.5197344	0.0143364	Response to stress
Adiponectin receptor 1	ADIPOR1	138982	1.1534308	1.1489419	0.0684965	Cell communication
F-box and leucine-rich repeat protein 11	FBXL11	134942	0.29659143	0.94774044	0.2516111	Cellular component organization
Golgi autoantigen, golgin subfamily a, 7	GOLGA7	138471	0.45656228	0.9966071	0.2516111	
CASP2 and RIPK1 domain containing adaptor with death domain	CRADD	24032	0.18224128	1.0878694	0.0855451	Cell communication, cell death
Inositol polyphosphate-4-phosphatase, type II, 105 kDa	INPP4B	165857	0.936418	1.2502048	0.0462351	Cell communication
HtrA serine peptidase 2	HTRA2	24797	0.72019017	1.7927532	0.0	Cellular component organization, cell death
Protein kinase, cAMP-dependent, regulatory, type I, beta	PRKAR1B	173325	1.475072	2.1799932	0.0	Cell communication
Chromatin assembly factor 1, subunit B (p60)	CHAF1B	35051	0.49089718	1.8564348	0.0	Cell cycle, cellular component organization
ATP-binding cassette, sub-family A (ABC1), member 7	ABCA7	182933	0.2530357	2.332722	0.0	Cellular component organization
Chaperonin containing TCP1, subunit 4 (delta)	CCT4	139688	0.3806577	1.5431345	0.0	Cell cycle
Dual specificity phosphatase 22	DUSP22	182999	0.25396538	1.9568335	0.0	Cell communication, cell proliferation, cell death
RNA binding motif, single stranded interacting protein 1	RBMS1	138929	0.8898407	1.0526701	0.2516111	Macromolecule metabolic process
Zinc finger, MIZ-type containing 1	ZMIZ1	24800	0.33787867	1.2721767	0.0440334	Regulation of biological process
Transformation/transcription domain-associated protein	TRRAP	21537	0.32666576	2.669969	0.0	Cell cycle, cellular component organization, cell communication
Sodium channel, voltage-gated, type II, beta	SCN2B	21485	0.3275153	2.9881008	0.0	Cell communication
Glutathione S-transferase pi	GSTP1	136235	0.2205719	4.2683134	0.0	Cell death

Table 1 continued

Name	Symbol	Clone ID	Expected Score (dExp)	Observed Score (d)	q-value (%)	Biological Process (GO[a])
SMAD family member 4	SMAD4	40768	0.5846094	0.830453	0.2516111	Cellular component organization, cell communication, cell proliferation
Calumenin	CALU	143860	0.46246096	1.2394656	0.0451074	
G protein-coupled receptor 34	GPR34	142865	0.2437603	2.36137	0.0	Cell communication
Thromboxane A synthase 1 (platelet, cytochrome P450, family 5, subfamily A)	TBXAS1	143443	0.391488	2.081456	0.0	Response to external stimulus, response to stress
Serpin peptidase inhibitor, clade H (heat shock protein 47), member 1, (collagen binding protein 1)	SERPINH1	142788	0.23954248	1.7802314	0.0	Macromolecule metabolic process, response to stress
S100 calcium binding protein P	S100P	135221	0.4515226	4.777696	0.0	Localization of cell
Solute carrier family 2 (facilitated glucose transporter), member 1	SLC2A1	25389	0.41978413	5.677428	0.0	Establishment of localization

[a] *GO gene ontology*

instability, thereby resulting in tumor development. On the other hand, the induction of genes related to cellular proliferation can also contribute to tumor progression. The *CALU* gene, for example, was up-regulated in the RT4 and T24 cell lines compared to the 5637 cell line. The increase in *CALU* expression suggests the transmission of accelerated cellular information [36], contributing to the uncontrolled cell proliferation observed in tumors.

Because the 5637 cell line presented different gene expression profiles than the other two cell lines, other genes and mechanisms involved in apoptosis and cell proliferation may be associated with bladder tumors. In agreement with the results of Hinata et al. [37], our qRT-PCR experiments showed that the *TP53* gene was highly expressed in the 5637 cells. Several authors have demonstrated that the nuclear accumulation of *p53* shows a high correlation with gene mutations [38]. Genes related to transcription, replication, and DNA synthesis were also observed to be differently expressed among the three cell lines. The up-regulation of *TRRAP, SUMO1, ZMIZ1,* and *RBMS1* in the 5637 cells might indicate stimulation of cell proliferation pathways that contribute to tumor development. *TRRAP* and *SUMO1* are important genes in the regulation of transcription [39, 40], while *ZMIZ1* acts in transcription and DNA replication and *RBMS1* is a DNA replication factor [41]. Moreover, death mechanisms were inhibited in the 5637 cells. The up-regulation of the *GSTP1, SMAD4,* and *CHAF1B* genes seems to block apoptosis and induce cell proliferation. Conversely, genes related to cell-cycle control were altered in the three cell lines. The *CHEK1* and *CCT4* genes were down- and up-regulated, respectively, in the 5637 cells. *CHEK1* is important in S phase and for the G2/M checkpoint [42]; meanwhile, *CCT4* is a positive regulator of the G1/S transition in the cell cycle [43]. Together, the data indicate that these checkpoints might be altered in tumoral cells.

Interestingly, the *TBXAS1* and *SLC2A1* genes were up-regulated in the RT4 cells. Several authors have shown that the *TBXAS1* up-regulation seems to be associated with advanced stages, high tumor grades and poor prognosis for patients with bladder cancer [44]. Additionally, high expression of *SLC2A1* in tumors has been associated with poor prognosis [45]. Based on our data, we believe that the use of these genes as potential tumor markers should be viewed carefully because high expression of these genes was also observed in the superficial tumor cell line. Conversely, *SERPINH1*, which regulates collagen production, was down-regulated in the *TP53*-mutated cells relative to the wild-type *TP53* cells. Some authors have found that *SERPINH1* is silenced in neuroblastoma cell lines [46]; in our study, this gene seemed be associated with the tumoral grade. The low-grade bladder tumor presented up-
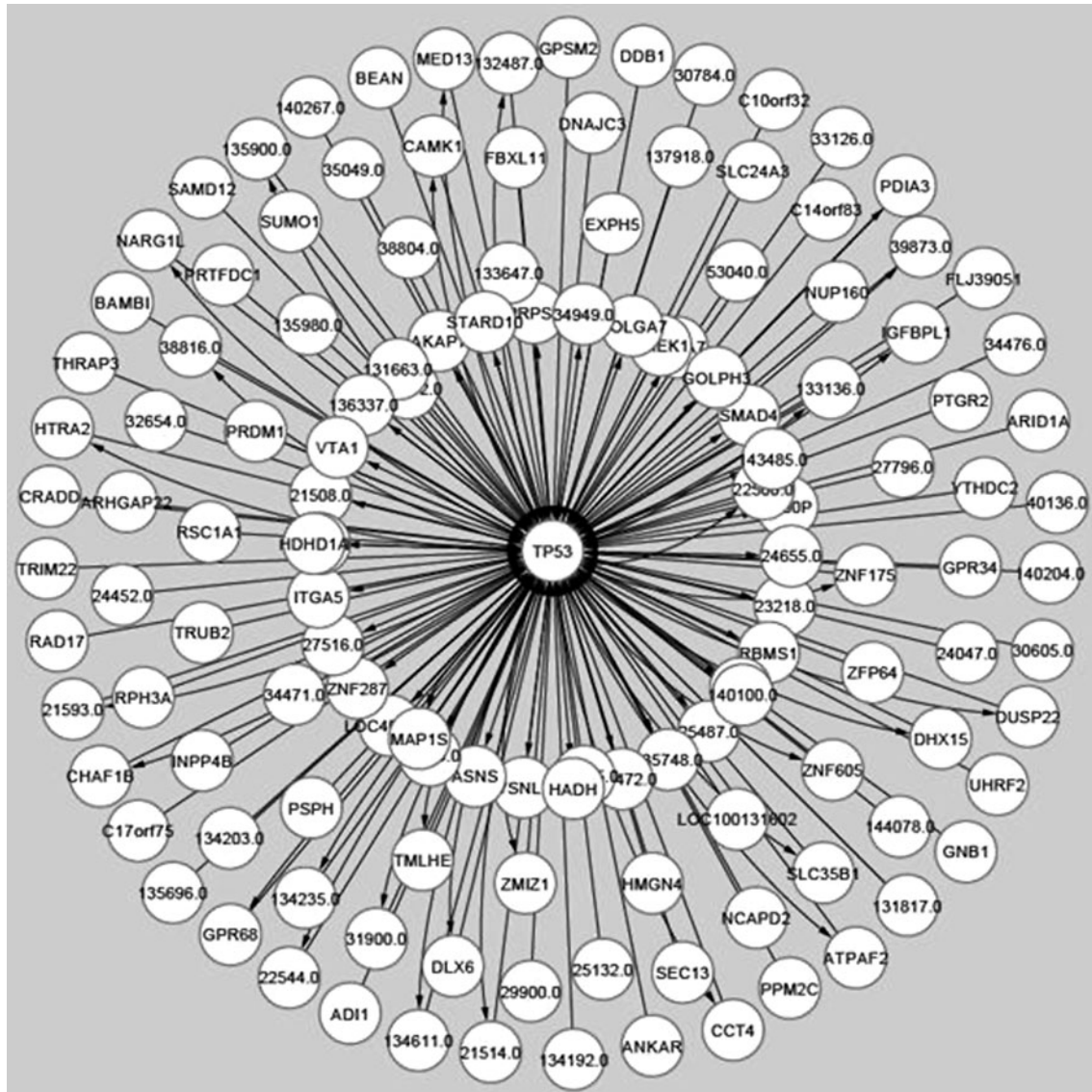
Fig. 2 Bayesian network of the RT4 × 5637 cell lines. The *TP53* transcript is in the center, and the probabilities of interactions with 182 other genes are shown

regulation of the *SERPINH1* expression, which could negatively influence the malignant potential of the RT4 cells.

In addition to the differences observed between the 5637 cells and the RT4 and T24 cells, it is important to note that the balance between cell proliferation and cell death involves several mechanisms and that, sometimes, the signal for cell survival surpasses signals for apoptosis. We observed different gene expression profiling in the three cell lines. Different genes associated with the inhibition of apoptosis and stimulation of cell proliferation were observed to be down- or up-regulated in the three lines, indicating that different mechanisms are involved in the development and progression of bladder cancer. Moreover, the divergence between the gene expression profiles of the 5637 and T24 cell lines, both of which have *TP53*

mutations, may reflect the complex biology of *TP53* in the regulation of apoptosis and cell proliferation. Because the *TP53* network is closely linked to many other cellular pathways, it is possible that defects in some of these pathways, either inherited or acquired somatically, could qualitatively or quantitatively interfere with the p53 function. Furthermore, p53 is only one component of the giant surveillance network whose efficiency is modulated by many other elements, including negative (Mdm2, Mdmx, Pirh2 and COP1) [47] and positive (DERP6) [48] regulators of p53, other members of the p53 family and several other signaling pathways [49].

Our data showed that the expression levels of *ANLN* and *S100P* as detected by qRT-PCR were significantly correlated with the mRNA expression levels observed in the

Fig. 3 Bayesian network of the RT4 × T24 cell lines. The *TP53* transcript is in the center, and the probabilities of interactions with 163 other genes are shown
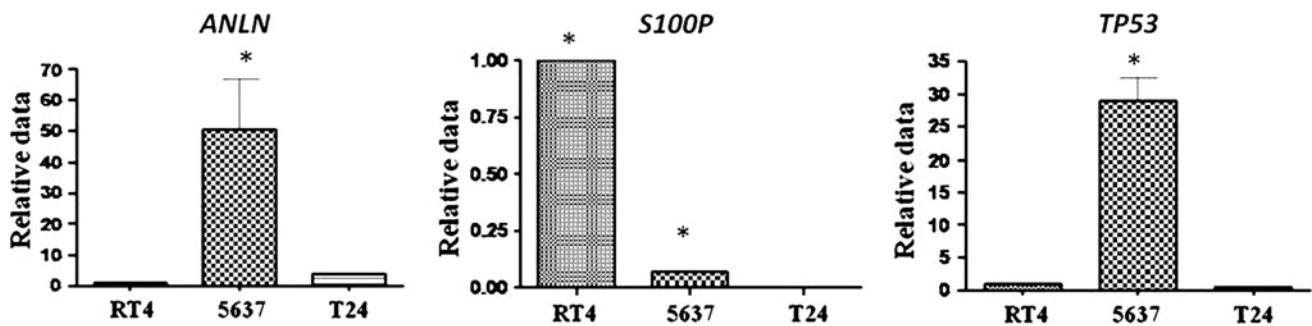

Fig. 4 Relative expression of the *ANLN*, *S100P*, and *TP53* genes. The RT4 cells had a relative expression value of 100. The data represent the mean and standard deviation for four independent experiments. *$P < 0.05$ when compared to the other two cell lines

cDNA microarray. The *S100P* gene encodes a calcium-binding protein expressed in different tumors that is functionally implicated in the malignant phenotype [50]. On the other hand, *ANLN* encodes the human homologue of anillin and plays an important role in cytokinesis [51]. We observed that the expression levels of *S100P* and *ANLN* were not associated with the tumor grade: *S100P* was significantly up-regulated in RT4 (low-grade superficial bladder tumor) compared to the 5637 and T24 cells, while *ANLN* was over-expressed in the cells from the grade 1 (RT4) and grade 3 (T24) tumors. Although the up-regulations of these two genes are important biomarkers for some tumors, our data showed lower expression of *S100P* in higher grade cells and *ANLN* in the RT4 and T24 cells. Therefore, *S100P* and *ANLN* expression levels should be carefully considered when planning therapeutic strategies for bladder cancer.

Conclusions

In conclusion, the molecular profiling using cDNA microarrays did not cluster the bladder cancer cell lines based on their *TP53* gene status. Our comprehensive expression profiling data can provide new insights into the molecular biology of bladder cancer. The identification of novel genetic susceptibility markers will help to understand the biology of urothelial carcinogenesis and may be integrated with clinical data and epidemiological and genetic risk factors for identifying individuals at high risk for developing bladder cancer.

Conflict of interest None.

References

1. Kirkali Z, Chan T, Manoharan M, Algaba F, Busch C, Cheng L, Kiemeney L, Kriegmair M, Montironi R, Murphy WM, Sesterhenn IA, Tachibana M, Weider J (2005) Bladder cancer: epidemiology, staging and grading, and diagnosis. Urology 66:4–34
2. Cookson MS, Herr W, Zhang ZF, Soloway S, Sogani PC, Fair WR (1997) The treated natural history of high risk superficial bladder cancer: 15-year outcome. J Urol 158:62–67
3. Nishiyama H, Habuchi T, Watanabe J, Teramukai S, Tada H, Ono Y, Ohshima S, Fujimoto K, Hirao Y, Fukushima M, Ogawa O (2004) Clinical outcome of a large-scale multi-institutional retrospective study for locally advanced bladder cancer: a survey including 1131 patients treated during 1990–2000 in Japan. Eur Urol 45:176–181
4. Cordon-Cardo C (2008) Molecular alterations associated with bladder cancer initiation and progression. Scand J Urol Nephrol Suppl 218:154–165
5. Wolff EM, Liang G, Jones PA (2005) Mechanisms of disease: genetic and epigenetic alterations that drive bladder cancer. Nat Clin Pract Urol 2:502–510
6. Levine A (2005) The p53 tumor-suppressor gene. N Engl J Med 1992(326):1350–1352
7. Sengupta S, Harris CC (2005) p53: traffic cop at the crossroads of DNA repair and recombination. Nat Rev Mol Cell Biol 6:44–55
8. Sanchez-Carbayo M, Socci ND, Charytonowicz E, Lu M, Prystowsky M, Childs G, Cordon-Cardo C (2002) Molecular profiling of bladder cancer using cDNA microarrays: defining histogenesis and biological phenotypes. Cancer Res 62:6973–6980
9. Sanchez-Carbayo M, Socci ND, Richstone L, Corton M, Behrendt N, Wulkfuhle J, Bochner B, Petricoin E, Cordon-Cardo C (2007) Genomic and proteomic profiles reveal the association of gelsolin to TP53 status and bladder cancer progression. Am J Pathol 171:1650–1658
10. Coppée J-Y (2008) Do DNA microarrays have their future behind them? Microbes Infect 10:1067–1071
11. Grant GR, Manduchi E, Stoeckert Jr CJ (2007) Analysis and management of microarray gene expression data. Curr Protoc Mol Biol, Chapter 19: Unit 19.6
12. Kraemer K, Schmidt U, Fuessel S, Herr A, Wirth MP, Meye A (2006) Microarray analyses in bladder cancer cells: inhibition of hTERT expression down-regulates EGFR. Int J Cancer 119:1276–1284
13. Kikuchi T, Daigo Y, Katagiri T, Tsunoda T, Okada K, Kakiuchi S, Zembutsu H, Furukawa Y, Kawamura M, Kobayashi K, Imai K, Nakamura Y (2003) Expression profiles of non-small cell lung cancers on cDNA microarrays: Identification of genes for prediction of lymph-node metastasis and sensitivity to anti-cancer drugs. Oncogene 22:2192–2205
14. Staege M, Banning-Eichenseer U, Weibflog G, Volkmer I, Burdach S, Richter G, Mauz-Korholz C, Foll J, Korholz D (2008) Gene expression profiles of Hodgkin's lymphoma cell lines with different sensitivity to cytotoxic drugs. Exp Hematol 36:886–896
15. Cooper MJ, Haluschak JJ, Johsond D, Schwartz S, Morrison LJ, Lippa M, Hatzivassiliou G, Tan J (1994) p53 mutations in bladder carcinoma cell lines. Oncol Res 6:569–579
16. Rieger KM, Little AF, Swart JM, Kastrinakis WV, Fitzgerald JM, Hess DT, Libertino JA, Summerhayes IC (1995) Human bladder carcinoma cell lines as indicators of oncogenic change relevant to urothelial neoplastic progression. Br J Cancer 72:683–690
17. da Silva GN, Marcondes JPC, Camargo EA, Passos GAS, Sakamoto-Hojo ET, Salvadori DMF (2010) Cell cycle arrest and apoptosis in TP53 subtypes of bladder carcinoma cell lines treated with cisplatin and gemcitabine. Exp Biol Med 235:814–824
18. Hegde P, Qi R, Abernathy K, Gay C, Dharap S, Gaspard R, Hughes JE, Snesrud E, Lee N, Quackenbush J (2000) A concise guide to cDNA microarray analysis. Biotechniques 29: 548–550, 552–544, 556 passim
19. Spot software [http://www.tm4.org/spotfinder.html]
20. Ihaka R, Gentleman R (1996) A language for data analysis and graphics. J Comput Graph Stat 5:299–314
21. KTH package [http://www.biotech.kth.se/molbio/microarray/]
22. Yang YH, Speed T (2002) Design issues for cDNA microarray experiments. Nat Rev Genet 3:579–588
23. MEV software [http://www.tm4.org/mev.html]
24. S.O.U.R.C.E. [http://smd-www.stanford.edu/cgi-bin/source/sourceSearch]
25. NCBI [http://www.ncbi.nlm.nih.gov/]
26. FATIGO [http://babelomics.bioinfo.cipf.es/]
27. Tusher VG, Tibshirani R, Chu G (2001) Significance analysis of microarrays applied to the ionizing radiation response. PNAS 98:5116–5121
28. Gene Network [http://idv.sinica.edu.tw/hchuang/GeneNetwork 1.2Setup.exe]

29. Blaveri E, Simko JP, James JE, Brewer JL, Baehner F, DeVries KS, Koppie T, Pejavar S, Carroll P, Waldman F (2005) Bladder cancer outcome and subtype classification by gene expression. Clin Cancer Research 11:4044–4055

30. Kato S (2003) Understanding the function structure and function mutation relationships of p53 tumor suppressor protein by high resolution missense mutation analysis. Proc Natl Acad Sci USA 100:8424–8429

31. Brosh R, Rotter V (2009) When mutations gain new powers: news from the mutant p53 field. Nat Rev Cancer 10:701–713

32. Prives C, Manfredi JJ (2005) The continuing saga of p53—More sleepless nighs ahead. Mol Cell 19:719–721

33. Zhao S, Zhang J, Zhang X, Dong X, Sun X (2008) Arsenic trioxide induces different gene expression profiles of genes related to growth and apoptosis in glioma cells dependent on the p53 status. Mol Biol Rep 35:421–429

34. Savopoulos JW, Carter PS, Turconi S, Pettman GR, Karran EH, Gray CW, Ward RV, Jenkins O, Creasy CL (2000) Expression, purification, and functional analysis of the human serine protease HtrA2. Protein Expr Purif 19:227–234

35. Muzio M, Stockwell BR, Stennicke HR, Salvesen GS, Dixit VM (1998) An induced proximity model for caspase-8 activation. J Biol Chem 273:2926–2930

36. Ding SJ, Li Y, Shao XX, Zhou H, Zeng R, Tang ZY, Xiav QC (2004) Proteome analysis of hepatocellular carcinoma cell strains, MHCC97-H and MHCC97-L, with different metastasis potentials. Proteomics 4:982–994

37. Hinata N, Shirakawa T, Zhang Z, Matsumoto A, Fujisawa M, Okada H, Kamidono S, Gotoh A (2003) Radiation induces p53-dependent cell apoptosis in bladder cáncer cells with wild-type-p53 but not in p53-mutated bladder cancer cells. Urol Res 31:387–396

38. Esrig D, Spruck CH 3rd, Nichols PW, Chaiwun B, Steven K, Groshen S, Chen SC, Skinner DG, Jones PA, Cote RJ (1993) p53 nuclear protein accumulation correlates with mutations in the p53 gene, tumor grade, and stage in bladder cancer. Am J Pathol 143:1389–1397

39. Fujita T, Kobayashi Y, Wada O, Tateishi Y, Kitada L, Yamamoto Y, Takashima H, Murayama A, Yano T, Baba T, Kato S, Kawabe Y-I, Yanagisawa J (2003) Full activation of estrogen receptor—activation function-1 induces proliferation of breast cancer cells. J Biol Chemistry 29:26704–26714

40. Hecker C-M, Rabiller M, Haglund K, Bayer P, Dikic I (2006) Specification of SUMO1- and SUMO2-interacting motifs. J Biol Chemistry 281:16117–16127

41. Niki T, Galli I, Ariga H, Iguchi-Ariga SMM (2000) MSSP, a protein binding to an origin of replication in the c-myc gene, interacts with a catalytic subunit of DNA polymerase α and stimulates its polymerase activity. FEBS Letters 475:209–212

42. Kortmansky J, Shah MA, Kaubisch A (2005) Phase I trial of thecyclin-dependent kinase inhibitor and protein kinase C inhibitor 7-hydroxystaurosporine in combination with fluorouracil in patients with advanced solid tumors. J Clin Oncol 23:1875–1884

43. Hart FU (1996) Molecular chaperones in cellular protein folding. Nature 381:571–579

44. Moussa O, Yordy JS, Abol-Enein H, Sinha D, Bissada NK, Haluska PV, Ghoneim MA, Watson DK (2005) Prognostic and functional significance of thromboxane synthase gene overexpression in invasive bladder cancer. Cancer Res 65:11581–11587

45. Macheda ML, Rogers S, Best JD (2005) Molecular and cellular regulation of glucose transporter (GLUT) proteins in cancer. J Cell Physiol 2202:654–662

46. Yang Q, Liu S, Tian Y, Hasan C, Kersey D, Salwen HR, Chlenski A, Perlman EJ, Cohn SL (2004) Methylation-associated silencing of the heat shock protein 47 gene in human neuroblastoma. Cancer Res 64:4531–4538

47. Wang L, He G, Zhang P, Wang X, Jiang M, Yu L (2010) Interplay between MDM2, MDMX, Pirh2 and COP1: the negative regulators of p53. Mol Biol Rep [Epub ahead of print]

48. Yuan J, Tang W, Luo K, Chen X, Gu X, Wan B, Yu L (2006) Cloning and characterization of the human gene DERP6, which activates transcriptional activities of p53. Mol Biol Rep 33:151–158

49. Soussi T, Wiman KG (2007) Shaping genetic alterations in human cancer: the p53 mutation paradigm. Cancer Cell 12:303–312

50. Guerreiro Da Silva IS, Hu YF, Russo IH, Ao X, Salicioni AM, Yang X, Russo J (2000) S100P calciumbinding protein overexpression is associated with immortalization of human breast epithelial cells in vitro and early stages of breast cancer development in vivo. Int J Oncol 16:231–240

51. Oegema K, Savoian MS, Matchinson TJ, Field CM (2000) Functional analysis of a human homologue of the Drosophila actin binding protein anillin suggests a role in cytokinesis. J Cell Biol 150:539–551